Exogenous insulin-like growth factor 1 attenuates cisplatin-induced muscle atrophy in mice

Hiroyasu Sakai[1]*, Maho Asami[1], Hiroaki Naito[1], Satoko Kitora[1], Yuta Suzuki[1], Yu Miyauchi[1], Rei Tachinooka[1], Satoshi Yoshida[1], Risako Kon[1], Nobutomo Ikarashi[1], Yoshihiko Chiba[2] & Junzo Kamei[1]

[1]*Department of Biomolecular Pharmacology, School of Pharmacy, Hoshi University, Tokyo, Japan;* [2]*Department of Physiology and Molecular Sciences, School of Pharmacy, Hoshi University, Tokyo, Japan*

Abstract

Background   A reduction in the skeletal muscle mass worsens the prognosis of patients with various cancers. Our previous studies indicated that cisplatin administration to mice caused muscle atrophy. This is a concern for human patients receiving cisplatin. The insulin-like growth factor 1 (IGF-1)/phosphoinositide 3-kinase (PI3K)/Akt pathway stimulates the rate of protein synthesis in skeletal muscle. Thus, IGF-I can be a central therapeutic target for preventing the loss of skeletal muscle mass in muscle atrophy, although it remains unclear whether pharmacological activation of the IGF-1/PI3K/Akt pathway attenuates muscle atrophy induced by cisplatin. In this study, we examined whether exogenous recombinant human IGF-1 attenuated cisplatin-induced muscle atrophy.

Methods   Male C57BL/6J mice (8–9 weeks old) were injected with cisplatin or saline for four consecutive days. On Day 5, quadriceps muscles were isolated. Mecasermin (recombinant human IGF-1) or the vehicle control was subcutaneously administered 30 min prior to cisplatin administration. A dietary restriction group achieving weight loss equivalent to that caused by cisplatin administration was used as a second control. C2C12 myotubes were treated with cisplatin with/without recombinant mouse IGF-1. The skeletal muscle protein synthesis/degradation pathway was analysed by histological and biochemical methods.

Results   Cisplatin reduced protein level of IGF-1 by about 85% compared with the vehicle group and also reduced IGF-1/PI3K/Akt signalling in skeletal muscle. Under this condition, the protein levels of muscle ring finger protein 1 (MuRF1) and atrophy gene 1 (atrogin-1) were increased in quadriceps muscles (MuRF1; 3.0 ± 0.1 folds, atrogin-1; 3.0 ± 0.3 folds, $P < 0.001$, respectively). The administration of a combination of cisplatin and IGF-1 significantly suppressed the cisplatin-induced downregulation of IGF-1/PI3K/Akt signalling and upregulation of MuRF1 and atrogin-1 (up to 1.6 ± 0.3 and 1.5 ± 0.4 folds, $P < 0.001$, respectively), resulting in diminished muscular atrophy. IGF-1 showed similar effects in cisplatin-treated C2C12 myotubes, as well as the quadriceps muscle in mice.

Conclusions   The downregulation of IGF-1 expression in skeletal muscle might be one of the factors playing an important role in the development of cisplatin-induced muscular atrophy. Compensating for this downregulation with exogenous IGF-1 suggests that it could be a therapeutic target for limiting the loss of skeletal muscle mass in cisplatin-induced muscle atrophy.

Keywords   Insulin-like growth factor 1; Cisplatin; Muscle atrophy; Mecasermin

Introduction

Cisplatin (also known as cisplatinum and cis-diamminedichloroplatinum(II); CDDP) combination chemotherapy is the basis of treatment of many cancers. Skeletal muscle is a very important tissue for human well-being and health.[1] Clinically, a loss of skeletal muscle mass deteriorates the prognosis of patients with various cancers such as ovarian cancer,[2] melanoma[3] and hepatocellular carcinoma.[4] Recently, Caan et al. indicated that sarcopenia occurred in one-third of new breast cancer patients, and similar to fat mass, it was a more robust predictor of death than the body mass index.[5] On the other hand, two muscle-specific ubiquitin E3–ubiquitin ligases have been discovered: muscle ring finger protein 1 (MuRF1) and atrophy gene 1 (atrogin-1)/muscle atrophy F-box.[6,7] Both MuRF1 and atrogin-1 are crucial components of the ubiquitin–proteasome proteolysis pathway and are significant mediators of protein degradation in skeletal muscle cells.[8] Under conditions of muscle atrophy, the expression levels of MuRF1 and atrogin-1 are significantly increased, and mice deficient in either gene are partially resistant to the development of skeletal muscle atrophy.[8] These results suggest that both molecules play a crucial role in muscle atrophy. MuRF1 and atrogin-1 are thus considered as specific markers of skeletal muscle atrophy (i.e. they are atrogenes).

Our previous studies indicated that cisplatin administration caused muscle atrophy in mice and that expression of MuRF1 and atrogin-1 is significantly increased under this condition.[9] In general, it is concerning for patients that cisplatin causes muscle atrophy, although the mechanism of cisplatin-induced muscle atrophy has not been fully elucidated. Thence, understanding the pathogenic mechanism of cisplatin itself-induced muscular atrophy and identifying new measures to prevent or reverse this effect are very important and urgent.

Muscle proteins constantly turn over by degradation and synthesis.[10] The balance between the rates of synthesis and degradation of muscle proteins (net muscle protein balance) determines the amount of protein in the muscle. Signalling pathways involving insulin-like growth factor 1 (IGF-1) and a cascade of intracellular components mediating its effects play major roles in regulating skeletal muscle growth.[11] IGF-1 enhances protein synthesis in skeletal muscle. When IGF-1 binds to its receptor, the complex phosphorylates the intracellular adapter protein, insulin receptor substrate 1 (IRS-1). This, in turn, phosphorylates phosphoinositide 3-kinase (PI3K), followed by Akt phosphorylation.

The PI3K/Akt signalling plays an important role in myotube hypertrophy,[12] and the activation/phosphorylation of Akt prevents atrophy induced by denervation in skeletal muscle of rat.[13] Mammalian target of rapamycin (mTOR) is activated in downstream target of PI3K/Akt signalling. The IGF-1/PI3K/Akt/mTOR pathway is indispensable in promoting muscle hypertrophy, and this boost in muscle mass improves the functional capacity of skeletal muscle.[14,15] mTOR, raptor, mLST8, PRAS40 and deptor compose mTOR complex 1 (mTORC1).[16] mTORC1 controls protein synthesis by activating/phosphorylating p70S6 kinase and inhibiting 4E-binding protein 1 (4E-BP1). By associating mRNA, p70S6 kinase and 4E-BP1 regulate the initiation and progression of translation and regulate the rate of protein synthesis. The IGF-1/PI3K/Akt/mTOR pathway ultimately increases the rate of protein synthesis via p70S6 kinase and p90 ribosomal S6 kinase while suppressing proteolysis primarily by its inhibitory effect on proteasome and lysosomal proteolysis.[17] IGF-I can be a central therapeutic target for preventing or reversing the reduction of skeletal muscle mass in muscle atrophy.[15] However, it remains unclear whether pharmacological stimulation of IGF-1/PI3K/Akt/mTOR signalling suppresses muscular atrophy induced by cisplatin. We determined whether exogenous IGF-1 could attenuate the muscle atrophy induced by cisplatin in this study.

Methods

Animals

Male C57BL/6J mice (8–9 weeks old, 23–27 g) were used in all animal experiments. The present study was conducted in accordance with the Guiding Principles for the Care and Use of Laboratory Animals, Hoshi University, as adopted by the Animal Research Committee of Hoshi University (Tokyo, Japan).

Administration schedule for cisplatin and mecasermin

Mice were administered once daily with cisplatin (3 mg/kg, intraperitoneally, FUJIFILM Wako Pure Chemical Corporation, Osaka, Japan) for 4 days using saline (vehicle) as a control. Because weight loss is caused by the suppression of food intake by cisplatin administration, we used dietary restriction (DR) as another control by performing pair feeding. Only 2, 2, 2 and 1.5 g meals were given to DR mice at Days 0–1, 1–2, 2–3 and 3–4, respectively. Mecasermin is a recombinant human IGF-1 designed for use as replacement therapy in severe primary IGF deficiency. Mecasermin (5 mg/kg, Somazon®, OrphanPacific, Inc. Tokyo, Japan) was subcutaneously injected 30 min before cisplatin. Twenty-four hours after the final injection of cisplatin (Day 3), animals were sacrificed under deep anaesthesia with overdose isoflurane inhalation, the femoral quadriceps muscles were removed, and their wet weights were measured.

Cell culture

C2C12 myoblast cells, derived from mouse striated muscle (RIKEN BRC, Ibaraki, Japan), were maintained in Dulbecco's modified Eagle's medium supplemented with 10% foetal calf serum, 0.1 mg/mL streptomycin and 100 U/mL penicillin at 37°C in an atmosphere of 95% air and 5% CO_2. When the cells reached 80% confluence, fusion and differentiation were initiated by replacing the medium with Dulbecco's modified Eagle's medium supplemented with 2% horse serum, 100 U/mL penicillin and 0.1 mg/mL streptomycin (differentiation medium). Cells were maintained in differentiation medium for 8 days prior to further experiments and were treated with cisplatin (5 or 15 μM) for 24 h in the presence or absence of 10 or 30 ng/mL IGF-1 (recombinant murine IGF-1, PeproTech, Rocky Hill, NJ, USA). The BCA protein assay (Protein Assay BCA Kit, Nacalai Tesque, Inc., Kyoto, Japan) was used for quantitation of protein concentration in the medium. Trichloroacetic acid (TCA) was then added to the medium to a final concentration of 15%. The TCA precipitation samples of medium were used for western blot. Cell Count Reagent SF (Nacalai Tesque, Inc.) was used to determine cell viability after being treated with 5 and 15 μM cisplatin for 24 h.

Western blots

The preparation of protein sample homogenate solutions and western blot analyses were performed as previously described.[18] The following primary rabbit antibodies were used: anti-IGF-1 (1:1000 dilution; PeproTech), anti-IGF-1R beta chain (1:1000 dilution; Proteintech Group, Inc., IL, USA), anti-MuRF1 (1:1000 dilution; ECM Biosciences, Versailles, KY, USA), anti-atrogin-1 (1:1000 dilution; ECM Biosciences), anti-Foxo3a (1:1000 dilution; Cell Signaling Technology, Danvers, MA, USA), anti-Akt (1:1000; Cell Signaling Technology), anti-phospho-Akt (1:1000; Cell Signaling Technology), anti-phospho-Foxo3a (1:1000; Cell Signaling Technology), anti-Smad2 (1:1000; Cell Signaling Technology) anti-phospho-Smad2/Smad3 (1:1000; Cell Signaling Technology),

and anti-phospho-Smad2 (1:1000; Cell Signaling Technology). The horseradish peroxidase-linked secondary antibodies used were goat anti-rabbit IgG (Cell Signaling Technology). In the examination of glyceraldehyde 3-phosphate dehydrogenase (GAPDH) protein levels, protein level of GAPDH relative to Ponceau-S staining was investigated.

Determination of IGF-1 levels

Murine IGF-1 levels were measured by a commercial Murine IGF-I Standard ABTS ELISA Development Kit according to the manufacturer's instructions (PeproTech).

Quantitative real-time polymerase chain reaction

For quantitative real-time polymerase chain reaction (qRT-PCR), quadriceps muscles were removed, washed with cold saline and stored in TRI Reagent™ (Sigma-Aldrich, St. Louis, MO, USA) at −80°C. The mRNA levels of various genes were examined using qRT-PCR as previously described.[18] Briefly, total RNA was extracted from femoral quadriceps muscles using a one-step guanidinium–phenol–chloroform extraction procedure with the TRI Reagent™ cDNAs prepared from total RNA (1.0 μg) using the ReverTra Ace qPCR RT Master Mix with gDNA Remover (Toyobo, Osaka, Japan). The diluted reaction mixture (2 μL) was subjected to PCR (50-nM forward and reverse primers, Fast SYBR Green Master Mix; Thermo Fisher Scientific, Waltham, MA, USA) in a final volume of 10 μL. The PCR primer sets used are shown in *Table* 1. The thermal cycle profile used was (1) denaturing for 30 s at 95°C and (2) annealing for 30 s at 60°C. PCR amplification was performed for 45 cycles. Data are presented as expression relative to GAPDH mRNA as a housekeeping gene using the $2^{-\Delta\Delta CT}$ method.

Histology

Haematoxylin and eosin staining and diameter measurements of the myofibres in quadriceps muscle were

Table 1 PCR primers used in the present study

	Accession no.		Primers	Product size (base pairs)
GAPDH	NM_008084.2	Forward	CCTCGTCCCGTAGACAAAATG	100
		Reverse	TCTCCACTTTGCCACTGCAA	
Atrogin-1	NM_026346.3	Forward	AGAAAAGCGGCAGCTTCGT	100
		Reverse	GCTGCGACGTCGTAGTTCAG	
MuRF1	NM_001039048.2	Forward	ACACAACCTCTGCCGGAAGT	103
		Reverse	ACGGAAACGACCTCCAGACA	
IGF-1	NM_010512.4	Forward	GACAGGCATTGTGGATGAGTGT	100
		Reverse	GATAGAGCGGGCTGCTTTTG	
IGF-1Ea (ref. [21])	NM_001111275.1	Forward	CTGACATGCCCAAGACTCAGAAGGA	72
		Reverse	AGGTCTTGTTTCCTGCACTTCCTCTAC	
IGF-1Eb (ref. [21])	NM_184052.3	Forward	GCCACACTGACATGCCCAAGA	123
		Reverse	CCGTTACCTCCTCCTGTTCCCC	

performed as previously described.[18] For each animal, at least 70 fibres were measured.

Immunohistochemistry

The quadriceps muscle was dissected out and post-fixed in 4% PFA in phosphate-buffered saline (PBS) for 1 h at 4°C. Samples were immersed in 30% sucrose/PBS overnight at 4°C and embedded in OCT compound (Sakura Finetek USA, Inc., Torrance, CA, USA). Frozen sections were cut with a cryostat (Leica Microsystems, Tokyo, Japan) at 10 μm and mounted onto MAS-coated glass slides (Matsunami Glass, Osaka, Japan). Sections were washed with PBS and blocked with blocking solution (PBS containing 3% serum and 0.1% Triton X-100) for 1 h; subsequently, sections were incubated overnight at 4°C in a mixture of primary antibody and rabbit anti-laminin (Sigma-Aldrich, 1:200). After washing three times with PBS, sections were reacted with secondary antibody (Alexa Fluor 488 anti-rabbit immunoglobulin G [IgG], Invitrogen Corp., Tokyo, Japan, 1: 300) at room temperature for 1 h. After washing with PBS, sections were reacted with 4,6-diamidino-2-phenylindole (DAPI) solution (Dojindo Laboratories, Kumamoto, Japan, 1: 2000) in PBS at room temperature for 30 min, washed three more times with PBS and then coverslipped with Vectashield (Vector Laboratories, Burlingame, CA, USA). Immunostained sections were observed under the fluorescence microscope FSX100 (Olympus Corporation, Tokyo, Japan) to measure the myofibre diameter of quadriceps muscles.

Statistical analyses

Data are presented as means ± standard deviation. The statistical significance of differences was determined using an unpaired Student's t-test or one-way analysis of variance with the Bonferroni/Dunn post hoc test. A $P < 0.05$ was considered significant.

Results

Effects of cisplatin on the expression of IGF-1 in mouse quadriceps muscles

The body weights of mice were significantly reduced to the same degree by the administration of cisplatin (3 mg/kg, intraperitoneally) and DR (Figure 1A). Under this condition, cisplatin treatment significantly decreased quadriceps muscle mass compared with that in the vehicle and DR groups (Figure 1B). To examine the expression of the IGF-1 gene in cisplatin-induced muscle atrophy, we performed qRT-PCR. The IGF-1 mRNA level in quadriceps muscle was significantly decreased by the administration of cisplatin compared with the vehicle and DR groups (Figure 1C). The IGF-1 protein is produced by different pre-propeptides, whereas two different promoters and differential splicing of the IGF-1 gene create several IGF-1 isoforms, which differ in the N-terminal signal peptide and the C-terminal extension peptide (E-peptide Ea or Eb; IGF-1Ea or Eb).[19–21] The IGF-1 primer used in this study amplifies both isoforms. The IGF-1Ea and IGF-1Eb gene expressions were examined using isoform-specific primers. The gene expressions of both isoforms were also significantly decreased by the administration of cisplatin compared with the vehicle and DR groups (Figure S1). Because the gene expression of IGF-1 was downregulated by cisplatin, we examined its protein level with western blotting. The protein level of IGF-1 in quadriceps muscle was significantly decreased by the administration of cisplatin compared with both the vehicle and DR groups (Figure 1D and 1E). Furthermore, there was a positive correlation between the quadriceps muscle mass and expression of IGF-1 protein (r = 0.803, $P < 0.01$; Figure 1F). We examined the plasma concentration of IGF-1. As a result of measuring plasma IGF-1 concentrations, no difference was observed among all groups (Figure 1G). Examination of IGF-1 levels in the quadriceps relative to the plasma IGF-1 concentrations showed a significant decrease with cisplatin administration compared with the vehicle and DR groups (Figure 1H). The protein levels of IGF-1 receptor (IGF-1R) were not changed by DR and cisplatin (Figure 1I and 1J). GAPDH was used as a housekeeping or normalization protein, because we showed that GAPDH was not changed by DR or cisplatin in muscle (Figure S2).

Effects of exogenous IGF-1 on the cisplatin-induced upregulation of MuRF1 and atrogin-1 in C2C12 myotubes

Although IGF-1 expression was decreased by cisplatin administration in vivo, whether cisplatin directly acted on skeletal muscle to cause this effect was unclear. We next examined the effect of cisplatin on IGF-1 expression in C2C12 myotubes. In these myotubes, the IGF-1 mRNA level was decreased by treatment with 15 μM cisplatin for 24 h compared with the vehicle group (Figure 2A), without altering cell viability (Figure S3). Similar to the qRT-PCR results, IGF-1 secreted into the medium was also significantly decreased in a concentration-dependent manner by cisplatin treatment compared with the vehicle group (Figure 2B). We investigated IGF-1 levels relative to Ponceau-S stained protein in medium or protein concentration of medium. In these studies, cisplatin also suppressed secreted IGF-1 in a concentration-dependent manner (Figure S4). In contrast, the expressions of the MuRF1 and atrogin-1 atrogenes were increased by cisplatin treatment. We investigated whether exogenous IGF could attenuate the cisplatin-induced
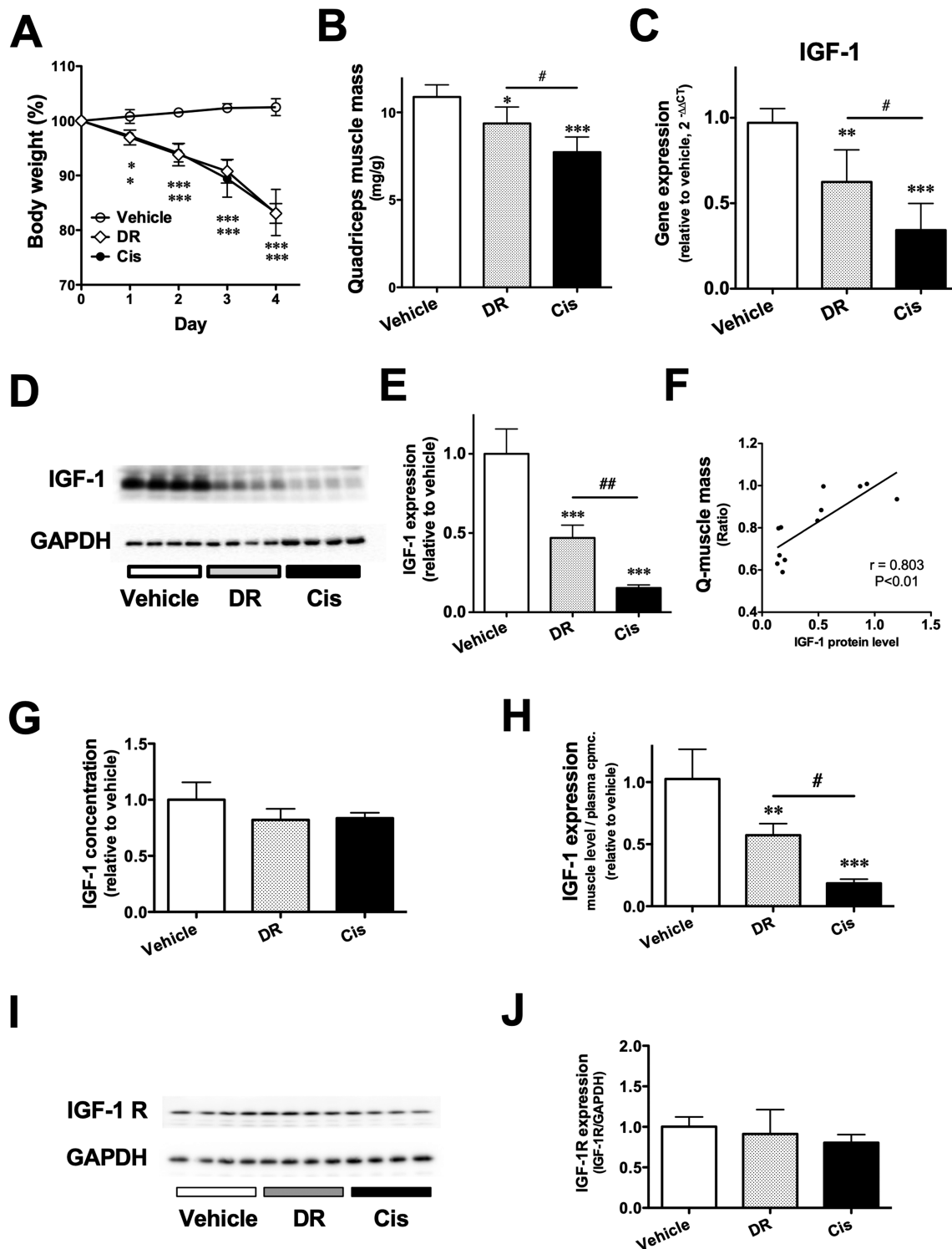
Figure 1 Cisplatin-induced downregulation of insulin-like growth factor 1 (IGF-1) expression in the quadriceps muscles of mice. Effects of 3 mg/kg cisplatin (Cis) and dietary restrictions (DR) on body weight *(A)* and quadriceps muscle mass *(B)*. Effects of DR and cisplatin on mRNA levels of IGF-1 in quadriceps muscle *(C)*. Representative photographs of western blot protein bands for IGF-1 and GAPDH *(D)*. Data are summarized in *(E)*. Correlation between muscle mass and protein levels of IGF-1 in quadriceps muscle (*F*, *r* = 0.803, *P* < 0.01). Effects of DR and cisplatin on plasma concentration of IGF-1. IGF-1 concentration in plasma was not changed by DR and cisplatin *(G)*. *(H)* IGF-1 levels in quadriceps muscle relative to IGF-1 concentration in plasma. Representative photographs of western blot protein bands for IGF-1 receptor (IGF-1R) and GAPDH *(I)*. Data are summarized in J. Each column represents the mean ± SD from four mice per group. *$P < 0.05$, **$P < 0.01$ and ***$P < 0.001$ vs. vehicle control (vehicle). #$P < 0.05$, ##$P < 0.01$ and ###$P < 0.01$ vs. DR.
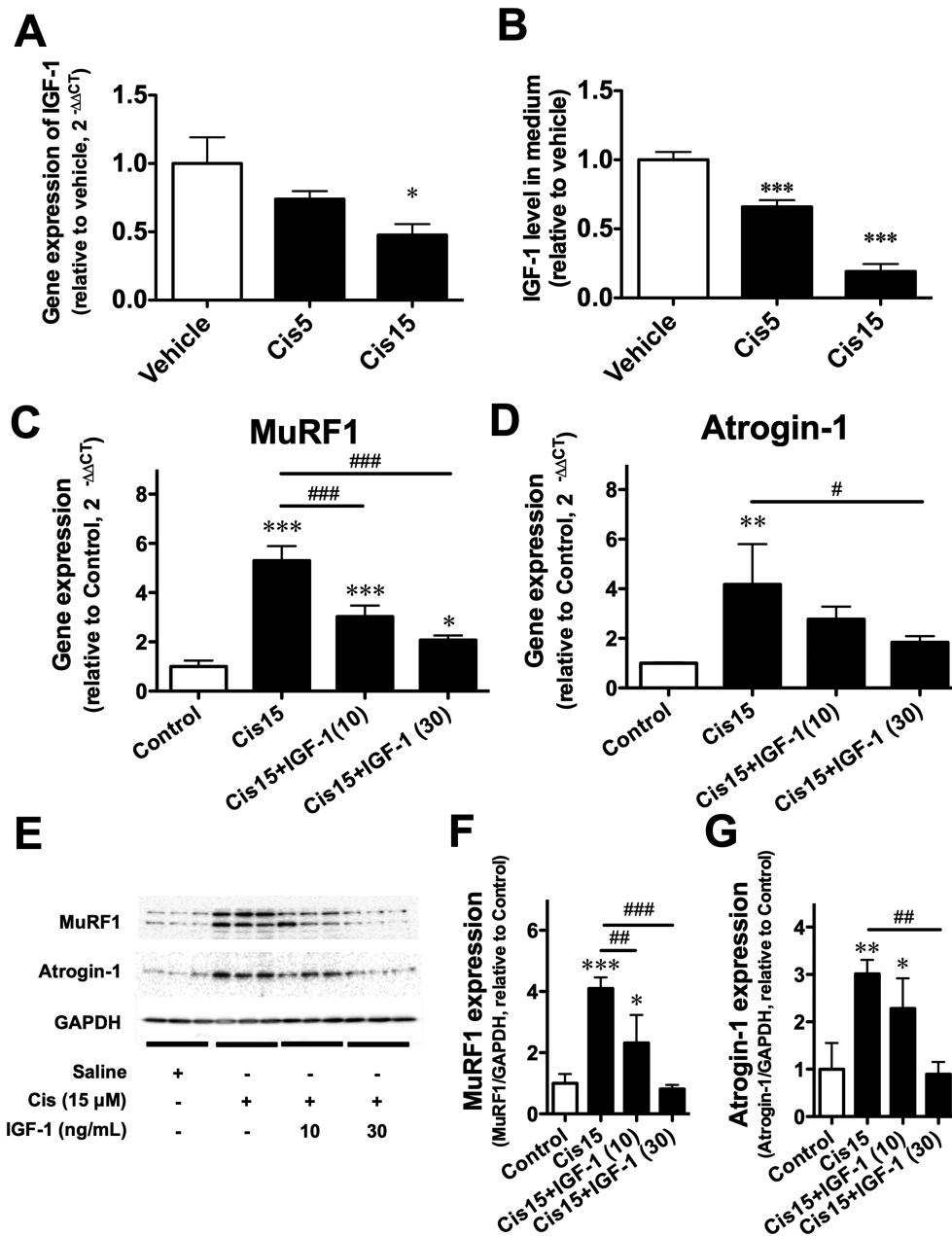
Figure 2 Effect of recombinant murine insulin-like growth factor-1 (IGF-1) on cisplatin-induced downregulation of IGF-1 expression in C2C12 myotubes. Effects of cisplatin (5 and 15 μM; Cis5 and Cis15, respectively) on IGF-1 mRNA levels *(A)* and secreted IGF-I protein levels *(B)* in C2C12 myotubes. Each column represents the mean ± SD from three independent experiments. *$P < 0.05$ and ***$P < 0.001$ vs. vehicle control (vehicle). Effects of IGF-1 on the mRNA levels of MuRF1 *(C)* and atrogin-1 *(D)* in C2C12 myotubes. Representative photographs of western blot bands for MuRF1, atrogin-1 and GAPDH proteins *(E)*. The data are summarized in *(F)* and *(G)*. Each column represents the mean ± SD from three independent experiments. *$P < 0.05$, **$P < 0.01$ and ***$P < 0.001$ vs. vehicle control (vehicle). #$P < 0.05$, ##$P < 0.01$ and ###$P < 0.001$ vs. Cis15.

upregulation of MuRF1 and atrogin-1 mRNAs and found that the changes induced by cisplatin treatment were significantly inhibited by exogenous IGF-1 treatment in a concentration-dependent manner (*Figure* 2C and 2D). Similarly, the cisplatin-induced increased in MuRF1 and atrogin-1 proteins was also attenuated by exogenous IGF-1 treatment (*Figure* 2E–G). GAPDH was also used as a house-keeping or normalized protein because it was shown that GAPDH was not altered by cisplatin or cisplatin + IGF-1 in the C2C12 myotube. (*Figure* S5A–C).

Effects of exogenous IGF-1 on cisplatin-induced changes of phosphorylation in C2C12 myotubes

The phosphorylation levels of Akt (*Figure* 3A and 3B), p70S6 kinase (*Figure* 3A and 3C) and Foxo3a (*Figure* 3D and 3E) were decreased by cisplatin. In contrast, Smad2/Smad3 and Smad2 phosphorylation was increased by cisplatin (*Figure* 3D and 3F). The reduction in Akt phosphorylation levels and the changes in Foxo3a and Smad2 phosphorylation levels by cisplatin treatment were suppressed by IGF treatment in concentration-dependent manners (*Figure* 3D–F).

Effects of mecasermin on cisplatin-induced muscle atrophy in mice

Mecasermin (recombinant human IGF-1) was administered to mice once daily for 4 days, 30 min before cisplatin treatment (*Figure* 4A). The body weight was not changed by mecasermin administration (*Figure* 4B). However, mecasermin significantly attenuated the cisplatin-induced loss of quadriceps muscle mass (*Figure* 4C). We then conducted a morphometric analysis of the quadriceps muscle with haematoxylin and eosin staining and
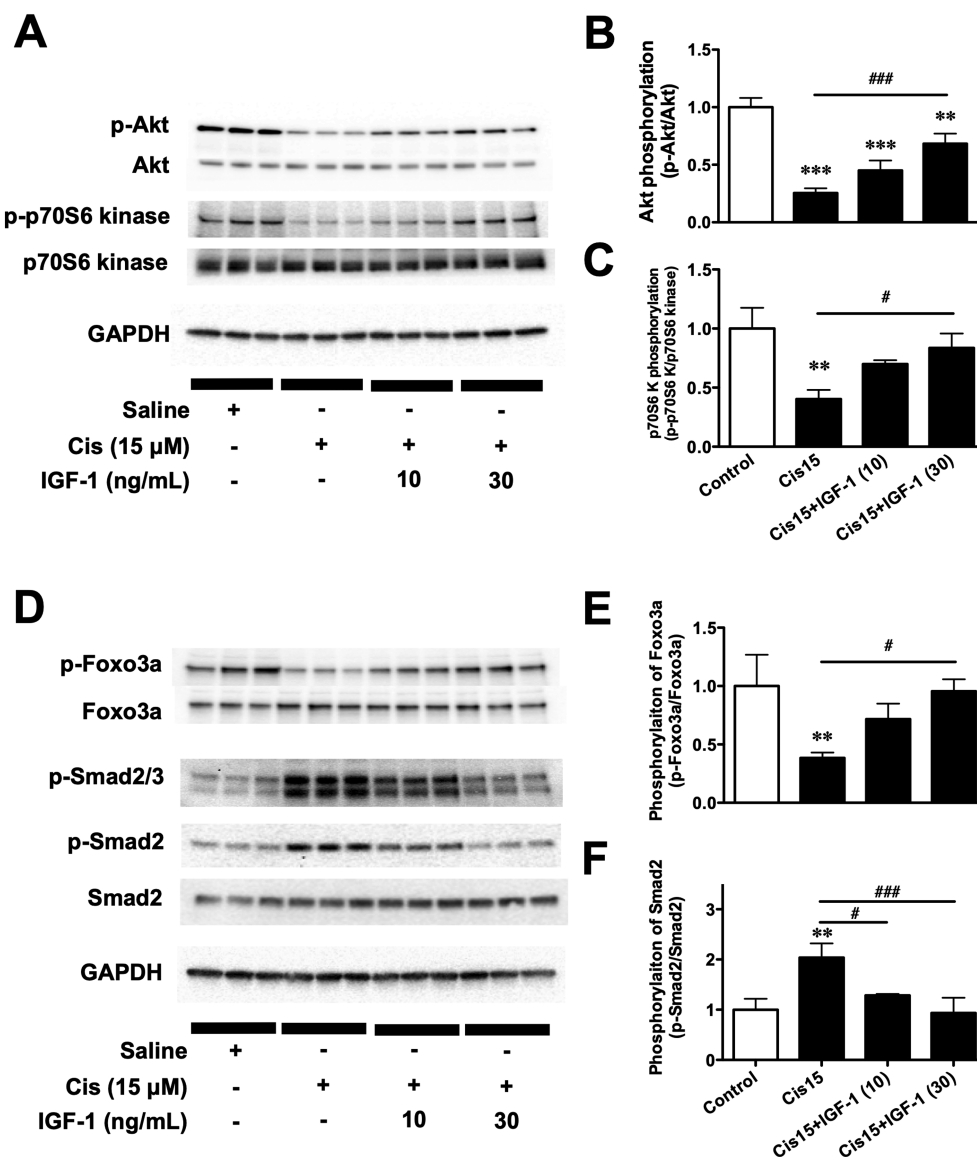

Figure 3 Effect of insulin-like growth factor-1 (IGF-1) on cisplatin-induced changes in IGF-1/Akt/mammalian target of rapamycin and Smad signalling in C2C12 myotubes. Representative photographs of western blot bands for phospho-Akt, total-Akt, phospho-p70S6 kinase, total-p70S6 kinase and GAPDH *(A)*. The data are summarized in *(B)* and *(C)*. Representative photographs of western blot bands for phospho-Foxo3a, total-Foxo3a, phospho-pSmad2/pSmad3, phospho-pSmad2, total-Smad2 and GAPDH *(D)*. Data are summarized in *(E)* and *(F)*. Each column represents the mean ± SD from three independent experiments. **$P < 0.01$ and ***$P < 0.001$ vs. vehicle control (control). #$P < 0.05$ and ###$P < 0.001$ vs. Cis15 (cisplatin 15 μM).
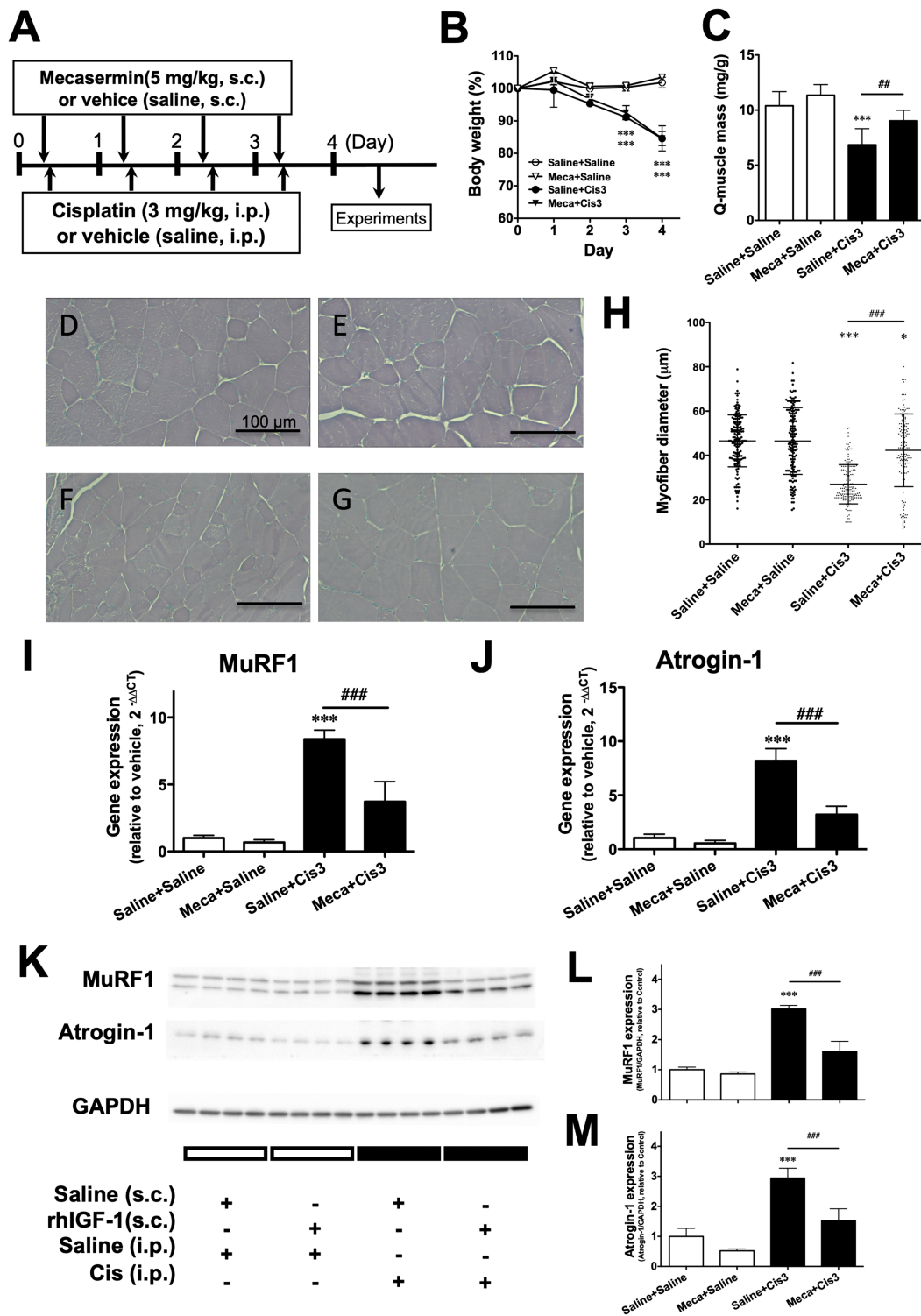
Figure 4 Effect of mecasermin (recombinant human insulin-like growth factor 1 [IGF-1]) on cisplatin-induced muscle atrophy in mice. Schedule for administration of the saline vehicle (intraperitoneally or subcutaneously), cisplatin (Cis3; 3 mg/kg, intraperitoneally) and mecasermin (Meca; 5 mg/kg, subcutaneously) (A). Effect of mecasermin on cisplatin-induced weight loss (B) and quadriceps muscle mass (C). Haematoxylin and eosin staining of quadriceps muscle in the Saline + Saline (D), Meca + Saline (E), Saline + Cis3 (F) and Meca + Cis3 (G). Bar scale = 100 μm. Effect of cisplatin and/or mecasermin on myofibre diameter (H). Effect of mecasermin on the cisplatin-induced upregulation of MuRF1 (I) and atrogin-1 (J) mRNA levels in mouse quadriceps muscle. Representative photographs of western blot bands for MuRF1, atrogin-1 and GAPDH (K). Data are summarized in (L) and (M). Each point and column represent the mean ± SD from four or five mice per group. *$P < 0.05$ and ***$P < 0.001$ vs. vehicle control (Saline + Saline). ##$P < 0.01$ and ###$P < 0.001$ vs. Saline + Cis3.

immunohistochemistry (*Figures* 4D–G and S6A–D). The decrease in myofibre diameter induced by cisplatin was significantly restored by mecasermin treatment (*Figures* 4H and S6E). Furthermore, the upregulation of MuRF1 and atrogin-1 mRNAs was also attenuated by mecasermin (*Figure* 4I and 4J). At the protein level, mecasermin showed similar effects (*Figure* 4K–M).

Effects of mecasermin on the cisplatin-induced changes of phosphorylation in mouse quadriceps muscle

The phosphorylation levels of Akt (*Figure* 5A and 5B), p70S6 kinase (*Figure* 5A and 5C) and Foxo3a (*Figure* 5D and 5E) in the quadriceps muscle were decreased by cisplatin. In contrast, Smad2/Smad3 and Smad2 phosphorylation was increased by cisplatin (*Figure* 5D and 5F). The reduction in Akt phosphorylation levels and the changes in Foxo3a and Smad2 phosphorylation by cisplatin treatment were suppressed by mecasermin administration (*Figure* 5E and 5F).

Discussion

In this study, we demonstrated that cisplatin treatment decreased IGF-1 levels and IGF-1 signalling in skeletal muscle and C2C12 myotubes. Under this treatment, the expression of MuRF1 and atrogin-1 was markedly increased. In this study, it was also shown that the administration of exogenous IGF-1 suppressed the cisplatin-induced upregulation of MuRF1 and atrogin-1, resulting in suppressed muscular atrophy.

In the IGF-1/PI3K/Akt pathway, the binding of IGF-1 to its receptor leads to the activation of its intrinsic tyrosine kinase and autophosphorylation, generating docking sites for IRS-1, which is also phosphorylated by the IGF-1 receptor. Phosphorylated IRS-1 then acts as a docking site to recruit and activate PI3K, which phosphorylates membrane phospholipids, generating phosphoinositide-3,4,5-trisphosphate from phosphoinositide-4,5-bisphosphate. Phosphoinositide-3,4,5-trisphosphate acts, in turn, as a docking site for two kinases, phosphoinositide-dependent kinase 1 and Akt, and the subsequent phosphorylation of Akt at serine 308 by phosphoinositide-dependent kinase 1, activates Akt. All these steps take place at the inner surface of the plasma membrane.

The IGF-1/PI3K/Akt/mTOR pathway is the primary driver of protein synthesis. Two biochemically and functionally distinct mTOR complexes exist: mTORC1 and mTORC2.[22] Downstream of mTORC1, two key proteins are activated to regulate muscle mass. A previous study has shown that mTORC1 signalling must both activate (phosphorylate) the p70S6 kinase and inhibit 4E-BP1 for an optimal amount and

quality of muscle mass during hypertrophic remodelling.[23] Akt inhibits protein degradation by phosphorylating, and repressing, transcription factors of the Foxo family and stimulates protein synthesis via mTOR and glycogen synthase kinase 3β.[11,24] Foxo factors are required for the transcriptional regulation of the ubiquitin ligases, MuRF1 and atrogin-1, leading to the ubiquitylation of muscle proteins and their subsequent degradation via the 26s proteasome, inducing muscle atrophy.[11]

We previously reported that IGF-1 gene expression in quadriceps muscle was decreased by cisplatin administration compared with vehicle control.[9] In the current study, this effect was confirmed and extended by showing that IGF-1 expression gene was significantly decreased by cisplatin administration compared both with the vehicle control and DR groups. Concomitant with the downregulation of IGF-1, the phosphorylation of Akt, p70S6 kinase and Foxo3a was decreased by cisplatin in mouse quadriceps muscle. These finding are also consistent with our previous study.[9] In another study, we found that the cisplatin-induced decreases in these phosphorylated forms in quadriceps muscle were attenuated by exercise loading with treadmill training and that this effect may be mediated by increased IGF-1 expression.[25]

When Foxo factors, chiefly Foxo3, are phosphorylated, they cannot translocate into the nucleus, and the expression of their target genes, MuRF1 and atrogin-1, is suppressed. It has been reported that when the IGF-1 expression decreases, Akt activity is suppressed and Foxo factors become dephosphorylated and translocate to the nucleus, increasing the expression of MuRF1 and atrogin-1 and enhancing protein degradation in skeletal muscle.[26–28]

The phosphorylated Smad2 or Smad3 can form a heterotrimeric complex with another Smad2 or Smad3 and a Smad4, and the resulting complex translocates into the nucleus to regulate gene transcription by associating with various transcription factors.[29] The activation of Smad signalling is reportedly sufficient to decrease protein synthesis, possibly by promoting atrogin-1-mediated degradation of ribosomal proteins and translation initiation factors or via the inhibition of signalling through the Akt/mTORC1 pathway.[30,31] Interestingly, cisplatin-induced downregulation of Smad2 phosphorylation was also attenuated by IGF-1. Studies with cancer cells have shown that the PI3K/Akt pathway and Smad signalling directly interact to isolate Smad3 outside the nucleus.[32] However, it has not yet been determined whether the same mechanism exists in skeletal muscle.

IGF-1 was previously thought of as a circulating growth factor that is produced primarily by the liver and mediates the effects of growth hormone on body growth. However, subsequent studies indicated that IGF-1 was also locally and significantly expressed in many tissues, including skeletal muscle, suggesting that autocrine/paracrine effects of local IGF-1 expression can be a crucial mechanism controlling tissue growth. To examine the effects of local IGF-1 produced
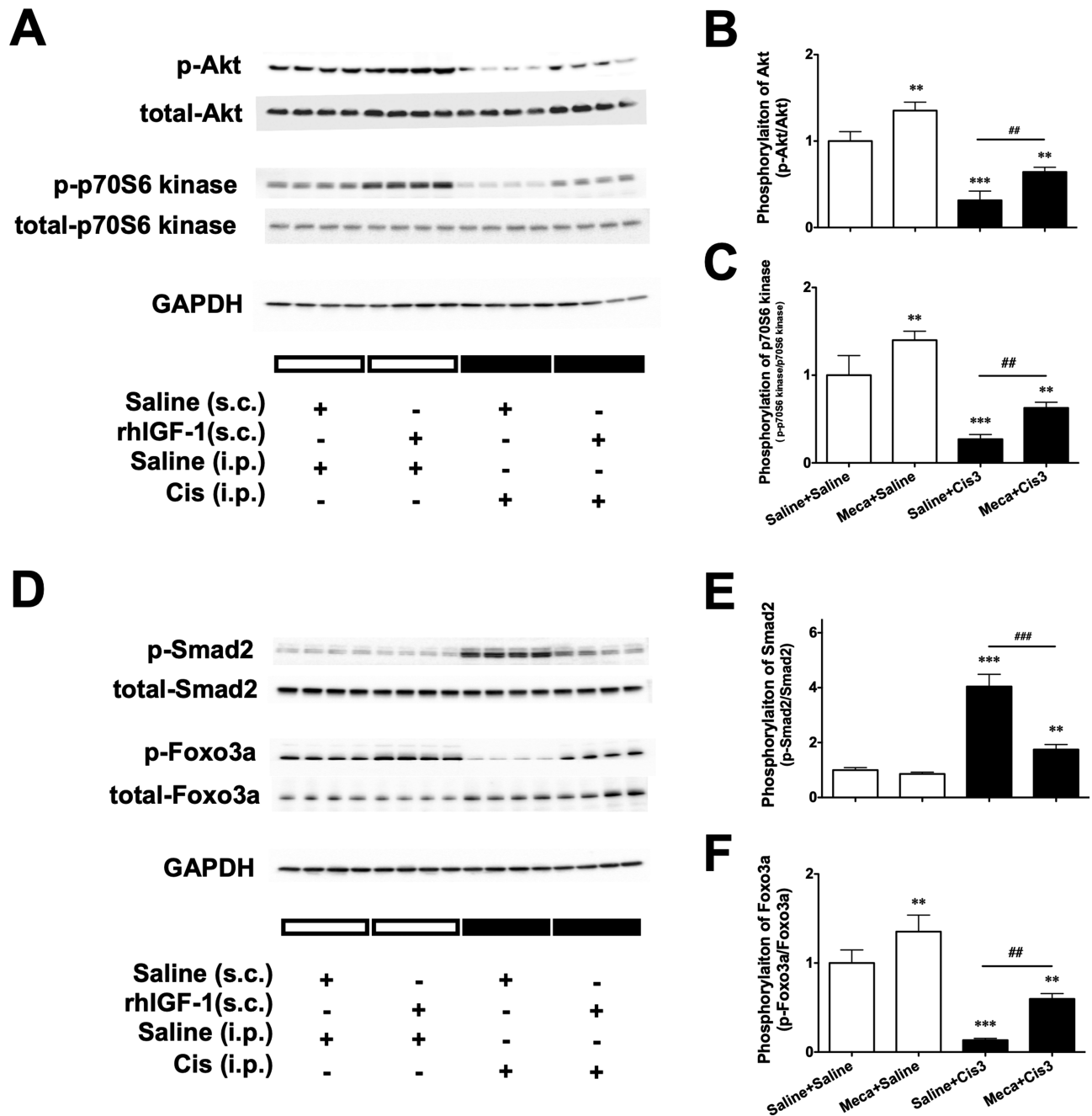
Figure 5 Effect of mecasermin on cisplatin-induced changes in insulin-like growth factor 1 (IGF-1)/Akt/mammalian target of rapamycin and Smad signalling in mouse quadriceps muscle. Representative photographs of western blot bands for phospho-Akt, total-Akt, phospho-p70S6 kinase, total-p70S6 kinase and GAPDH (A). Data are summarized in (B) and (C). Representative photographs of western blot bands for phospho-Foxo3a, total-Foxo3a, phospho-pSmad2, total-Smad2 and GAPDH (D). Data are summarized in (E) and (F). Each column represents the mean ± SD from four or five mice per group. **$P < 0.01$ and ***$P < 0.001$ vs. vehicle control (Saline + Saline). #$P < 0.05$ and ###$P < 0.001$ vs. Saline + Cis3 (cisplatin 3 mg/kg).

by muscle cells, a transgenic construct was generated in which the expression of a human IGF-1 cDNA was driven by the avian skeletal α-actin gene.[11,33] The resultant transgenic mice developed skeletal muscle hypertrophy.[33–35] In the transgenic mice, IGF-1 overexpression was not sufficient to prevent the decrease in muscle mass induced by hind-limb unloading.[34] However, glucocorticoid-induced muscle atrophy was prevented by IGF-1 overexpression via electroporation in adult rats.[36] This was consistent with the results of the current study showing that cisplatin-induced muscle atrophy was improved by exogenous IGF-1. However, administration of IGF-1 to cancer patients is contraindicated in

clinical practice, because IGF-1 can exacerbate cancer. In addition, Jeon et al.[37] have shown that IGF-1 counteracts the anti-neoplastic effect of cisplatin. Unfortunately, the findings in this study cannot directly link to clinical therapy, and systemic administration of IGF-1 is likely to exacerbate cancer. In the study of Duchenne muscular dystrophy, therapeutic studies using adeno-associated virus (AAV) vectors are being actively conducted.[38–40] Similarly, integration of a skeletal muscle-specific promoter into an AAV vector enhances expression of IGF-1 in skeletal muscle. This technique may suppress cisplatin-induced muscle atrophy, although a lot of preliminary research is needed. In addition, the search for new factors and methods that locally activate PI3K/Akt/mTOR signalling in only skeletal muscle may become new therapeutic targets for the treatment of cisplatin-induced muscle atrophy in the future.

In conclusion, the downregulation of IGF-1 expression in skeletal muscle might be one of the factors playing an important role in the development of cisplatin-induced muscular atrophy in mouse. The ability to compensate for this loss by the administration of exogenous IGF-1 suggests that this could be a therapeutic approach for preventing or reversing the loss of skeletal muscle mass in cisplatin-induced muscle atrophy.

Acknowledgements

Funding

Online supplementary material

Additional supporting information may be found online in the Supporting Information section at the end of the article.

Figure S1. Effects of DR and cisplatin on mRNA levels of IGF-1Ea (A) and IGF-1Eb (B) in quadriceps muscle of mouse. Each column represents the mean ± SD from four mice per group. $*P < 0.05$ and $***P < 0.001$ vs. vehicle control (Vehicle). $^{##}P < 0.01$, and $^{###}P < 0.01$ vs. DR.

Figure S2. Effect of dietary restrictions, cisplatin (3 mg/kg), mecasermin (5 mg/kg) and their combination on the protein levels of GAPDH in quadriceps muscle. A and D show representative Ponceau-S staining. B and E show representative immunoblot for GAPDH. M.M.; molecular weight marker. C and F show expression levels of GAPDH relative to Ponceau-S staining. Each column represents the mean ± SD from four mice per group. GAPDH expressions were not changed among all groups.

Figure S3. Effects of cisplatin (5 and 15 μM for 24 hr) on the cell viability in C2C12 myotubes. Each column represents the mean ± SD from six independent samples.

Figure S4. Effect of cisplatin (5 and 15 μM) on the IGF-1 levels in trichloroacetic acid (TCA) precipitation of proteins from medium of C2C12 myotubes. A shows representative Ponceau-S staining. M.M; molecular weight marker. B shows representative immunoblot for IGF-1. C shows the levels IGF-1 relative to Ponceau-S staining. The levels of IGF-1 relative to each protein concentration are shown in D. Each column represents the mean ± SD from three independent samples per group. The protein levels of IGF-1 were not changed among all groups.

Figure S5. Effects of cisplatin (5 μM) + IGF-1 (10 or 30 ng/mL) on the protein levels of GAPDH in C2C12 myotubes. A shows representative Ponceau-S staining. B shows representative immunoblot for GAPDH. M.M; molecular weight marker. C and F shows expression levels of GAPDH relative to Ponceau-S staining. Each column represents the mean ± SD from three independent samples per group. The protein levels of GAPDH were not changed at all groups.

Figure S6. Effects of cisplatin and mecasermin on the myofiber diameter. Immunofluorescence staining for laminin of quadriceps muscle in the Saline + Saline (A), Meca +Saline (B), Saline+ Cis3 (C), aBMD Meca + Cis3 (D). Bar scale = 100 μm. The diameter is shown in E. Each point and column represent the mean ± SD from three mice per group. $**p < 0.01$ and $***P < 0.001$ vs. vehicle control (Saline + Saline). $^{###}P < 0.001$ vs. Saline + Cis3.

Conflict of interest

None declared.

Ethical statement

The present study was conducted in accordance with the Guiding Principles for the Care and Use of Laboratory Animals, Hoshi University, as adopted by the Animal Research Committee of Hoshi University (Tokyo, Japan).

References

1. Wolfe RR. The underappreciated role of muscle in health and disease. *Am J Clin Nutr* 2006;**84**:475–482.
2. Aust S, Knogler T, Pils D, Obermayr E, Reinthaller A, Zahn L, et al. Skeletal muscle depletion and markers for cancer cachexia are strong prognostic factors in epithelial ovarian cancer. *PLoS ONE* 2015;**10**: e0140403.
3. Sabel MS, Lee J, Cai S, Englesbe MJ, Holcombe S, Wang S. Sarcopenia as a prognostic factor among patients with stage III melanoma. *Ann Surg Oncol* 2011;**18**: 3579–3585.
4. Fujiwara, Nakagawa H, Kudo Y, Tateishi R, Taguri M, Watadani T, et al. Sarcopenia, intramuscular fat deposition, and visceral adiposity independently predict the outcomes of hepatocellular carcinoma. *J Hepatol* 2015;**63**:131–140.
5. Caan BJ, Cespedes Feliciano EM, Prado CM, Alexeeff S, Kroenke CH, Bradshaw P, et al. Association of muscle and adiposity measured by computed tomography with survival in patients with nonmetastatic breast cancer. *JAMA Oncol* 2018;**4**: 798–804.
6. Bodine SC, Latres E, Baumhueter S, Lai VK, Nunez L, Clarke BA, et al. Identification of ubiquitin ligases required for skeletal muscle atrophy. *Science* 2001;**294**: 1704–1708.
7. Gomes, Lecker SH, Jagoe RT, Navon A, Goldberg AL. Atrogin-1, a muscle-specific F-box protein highly expressed during muscle atrophy. *Proc Natl Acad Sci U S A* 2001;**98**:14440–14445.
8. Bodine SC, Baehr LM. Skeletal muscle atrophy and the E3 ubiquitin ligases MuRF1 and MAFbx/atrogin-1. *Am J Physiol Endocrinol Metab* 2014;**307**:E469–E484.
9. Sakai H, Sagara A, Arakawa K, Sugiyama R, Hirosaki A, Takase K, et al. Mechanisms of cisplatin-induced muscle atrophy. *Toxicol Appl Pharmacol* 2014;**278**:190–199.
10. Tipton KD, Hamilton DL, Gallagher IJ. Assessing the role of muscle protein breakdown in response to nutrition and exercise in humans. *Sports Med* 2018;**48**: 53–64.
11. Schiaffino S, Mammucari C. Regulation of skeletal muscle growth by the IGF1-Akt/PKB pathway: insights from genetic models. *Skelet Muscle* 2011;**1**:4.
12. Rommel C, Bodine SC, Clarke BA, Rossman R, Nunez L, Stitt TN, et al. Mediation of IGF-1-induced skeletal myotube hypertrophy by PI(3)K/Akt/mTOR and PI(3)K/Akt/GSK3 pathways. *Nat Cell Biol* 2001;**3**: 1009–1013.
13. Pallafacchina G, Calabria E, Serrano AL, Kalhovde JM, Schiaffino S. A protein kinase B-dependent and rapamycin-sensitive pathway controls skeletal muscle growth but not fiber type specification. *Proc Natl Acad Sci U S A* 2002;**99**:9213–9218.
14. Glass DJ. PI3 kinase regulation of skeletal muscle hypertrophy and atrophy. *Curr Top Microbiol Immunol* 2010;**346**:267–278.
15. Yoshida T, Delafontaine P. Mechanisms of IGF-1-mediated regulation of skeletal muscle hypertrophy and atrophy. *Cell* 2020;**9**:1970.
16. Beauchamp EM, Platanias LC. The evolution of the TOR pathway and its role in cancer. *Oncogene* 2013;**32**:3923–3932.
17. Ma XM, Blenis J. Molecular mechanisms of mTOR-mediated translational control. *Nat Rev Mol Cell Biol* 2009;**10**:307–318.
18. Sakai H, Kimura M, Tsukimura Y, Yabe S, Isa Y, Kai Y, et al. Dexamethasone exacerbates cisplatin-induced muscle atrophy. *Clin Exp Pharmacol Physiol* 2019;**46**:19–28.
19. Shavlakadze T, Winn N, Rosenthal N, Grounds MD. Reconciling data from transgenic mice that overexpress IGF-I specifically in skeletal muscle. *Growth Horm IGF Res* 2005;**15**:4–18.
20. Ascenzi F, Barberi L, Dobrowolny G, Villa Nova Bacurau A, Nicoletti C, Rizzuto E, et al. Effects of IGF-1 isoforms on muscle growth and sarcopenia. *Aging Cell* 2019;**18**:e12954.
21. Nielsen RH, Clausen NM, Schjerling P, Larsen JO, Martinussen T, List EO, et al. Chronic alterations in growth hormone/insulin-like growth factor-I signaling lead to changes in mouse tendon structure. *Matrix Biol* 2014;**34**:96–104.
22. Laplante M, Sabatini DM. mTOR signaling in growth control and disease. *Cell* 2012;**149**:274–293.
23. Marabita M, Baraldo M, Solagna F, Ceelen JJM, Sartori R, Nolte H, et al. S6K1 is required for increasing skeletal muscle force during hypertrophy. *Cell Rep* 2016;**17**: 501–513.
24. Manning BD, Cantley LC. AKT/PKB signaling: navigating downstream. *Cell* 2007;**129**:1261–1274.
25. Sakai H, Kimura M, Isa Y, Yabe S, Maruyama A, Tsuruno Y, et al. Effect of acute treadmill exercise on cisplatin-induced muscle atrophy in the mouse. *Pflugers Arch* 2017;**469**:1495–1505.
26. Sandri M, Sandri C, Gilbert A, Skurk C, Calabria E, Picard A, et al. Foxo transcription factors induce the atrophy-related ubiquitin ligase atrogin-1 and cause skeletal muscle atrophy. *Cell* 2004;**117**:399–412.
27. Bonaldo P, Sandri M. Cellular and molecular mechanisms of muscle atrophy. *Dis Model Mech* 2013;**6**:25–39.
28. Milan G, Romanello V, Pescatore F, Armani A, Paik JH, Frasson L, et al. Regulation of autophagy and the ubiquitin-proteasome system by the FoxO transcriptional network during muscle atrophy. *Nat Commun* 2015;**6**:6670.
29. Ross S, Hill CS. How the Smads regulate transcription. *Int J Biochem Cell Biol* 2008;**40**:383–408.
30. Trendelenburg AU, Meyer A, Rohner D, Boyle J, Hatakeyama S, Glass DJ. Myostatin reduces Akt/TORC1/p70S6K signaling, inhibiting myoblast differentiation and myotube size. *Am J Physiol Cell Physiol* 2009;**296**:C1258–C1270.
31. Hulmi JJ, Oliveira BM, Silvennoinen M, Hoogaars WM, Ma H, Pierre P, et al. Muscle protein synthesis, mTORC1/MAPK/Hippo signaling, and capillary density are altered by blocking of myostatin and activins. *Am J Physiol Endocrinol Metab* 2013;**304**:E41–E50.
32. Zhang L, Zhou F, ten Dijke P. Signaling interplay between transforming growth factor-beta receptor and PI3K/AKT pathways in cancer. *Trends Biochem Sci* 2013;**38**:612–620.
33. Coleman ME, DeMayo F, Yin KC, Lee HM, Geske R, Montgomery C, et al. Myogenic vector expression of insulin-like growth factor I stimulates muscle cell differentiation and myofiber hypertrophy in transgenic mice. *J Biol Chem* 1995;**270**: 12109–12116.
34. Criswell DS, Booth FW, DeMayo F, Schwartz RJ, Gordon SE, Fiorotto ML. Overexpression of IGF-I in skeletal muscle of transgenic mice does not prevent unloading-induced atrophy. *Am J Physiol* 1998;**275**:E373–E379.
35. Fiorotto ML, Schwartz RJ, Delaughter MC. Persistent IGF-I overexpression in skeletal muscle transiently enhances DNA accretion and growth. *FASEB J* 2003;**17**:59–60.
36. Schakman O, Gilson H, de Coninck V, Lause P, Verniers J, Havaux X, et al. Insulin-like growth factor-I gene transfer by electroporation prevents skeletal muscle atrophy in glucocorticoid-treated rats. *Endocrinology* 2005;**146**:1789–1797.
37. Jeon JH, Kim SK, Kim HJ, Chang J, Ahn CM, Chang YS. Insulin-like growth factor-1 attenuates cisplatin-induced gammaH2AX formation and DNA double-strand breaks repair pathway in non-small cell lung cancer. *Cancer Lett* 2008;**272**:232–241.
38. Mendell JR, Al-Zaidy SA, Rodino-Klapac LR, Goodspeed K, Gray SJ, Kay CN, et al. Current clinical applications of in vivo gene therapy with AAVs. *Mol Ther* 2021;**29**: 464–488.
39. Flotats-Bastardas M, Hahn A. New therapeutics options for pediatric neuromuscular disorders. *Front Pediatr* 2020;**8**: 583877.
40. Li C, Samulski RJ. Engineering adeno-associated virus vectors for gene therapy. *Nat Rev Genet* 2020;**21**:255–272.
41. von Haehling S, Morley JE, Coats AJS, Anker SD. Ethical guidelines for publishing in the journal of cachexia, sarcopenia and muscle: update 2019. *J Cachexia Sarcopenia Muscle* 2019;**10**:1143–1145.